

Landmarks for rapid localization of the sphenopalatine foramen: A radiographic morphometric analysis

Anne K. Maxwell, M.D., Henry P. Barham, M.D., Anne E. Getz, M.D., Todd T. Kingdom, M.D., and Vijay R. Ramakrishnan, M.D.

ABSTRACT

Background: Transnasal endoscopic sphenopalatine artery ligation is becoming the procedure of choice for surgical management of intractable posterior epistaxis. Landmarks for localization of the sphenopalatine foramen can assist in rapid surgical exposure of the sphenopalatine artery.

Objective: This study examined distances from easily identified endoscopic surgical landmarks to the sphenopalatine foramen.

Methods: By using computed tomography of the sinus to study radiologic anatomy in 50 adults, distances were measured between five simple endoscopic landmarks and the sphenopalatine foramen. The two-tailed *t*-test was used for statistical analysis.

Results: Right- and left-sided measurements were similar. The mean (standard deviation [SD]) anteroposterior distances to the sphenopalatine foramen were the following: from the maxillary line (36.7 ± 5.5 mm), anterior head of the middle turbinate (33.8 ± 6.7 mm), basal lamella (11.8 ± 1.9 mm), and choanal arch (-9.2 ± 1.4 mm). The mean (SD) distance in the vertical dimension from the nasal floor was 26.6 ± 2.6 mm. Female patients had statistically shorter distances to the sphenopalatine foramen from the maxillary line, anterior head of the middle turbinate, choanal arch, and nasal floor.

Conclusion: Reliable endoscopic landmarks exist in relation to consistent anatomic structures and can be used to help quickly estimate the location of the sphenopalatine foramen at the onset of the procedure.

(Allergy Rhinol 8:e63–e66, 2017; doi: 10.2500/ar.2017.8.0196)

Epistaxis is the most common otolaryngologic emergency, which occurs in ~10% of the population.^{1–3} More than 90% of epistaxis cases originate anteriorly from the Kiesselbach plexus over the anterior nasal septum.^{1,4} However, most severe intractable cases arise posteriorly. The sphenopalatine artery (SPA), a terminal branch of the internal maxillary artery (IMA), supplies blood to the lateral nasal wall, inferior and middle turbinate, and the posterior septum, and is implicated in most cases of posterior epistaxis.^{1,4} Most epistaxis cases can be conservatively controlled with nasal packing or direct cautery; however, intractable cases usually proceed to arterial ligation or embolization of the SPA or distal IMA.

Arterial ligation at proximal sites (e.g., the external carotid or IMA) generally carries higher failure rates

than distal ligation due to the presence of collateral circulation and anastomoses.⁵ When addressing the key distal branch of the relevant external carotid circulation, transnasal endoscopic SPA ligation (TESPAL) has become the procedure of choice for intractable epistaxis due to its efficacy, favorable risk-benefit ratio, and cost-effectiveness.^{4,6,7} TESPAL typically does not require dissection of the sinuses, and a direct approach to the SPA would be ideal. The location of the sphenopalatine foramen (SPF) is identified within the superior meatus after elevation of a mucoperiosteal flap and identification of the crista ethmoidalis from the posterior aspect of the middle meatus. Opening the maxillary sinus may assist the surgeon if these landmarks are not quickly found. Difficulty in locating the SPA as it exits the SPF may be compounded by active bleeding that obscures the operative field or edematous and friable tissue caused by previous nasal packing. As such, the addition of simple surgical landmarks to locate the SPF would be helpful beyond the traditional reliance on the crista ethmoidalis. The aim of this study was to determine if simple endonasal anatomic relationships exist to facilitate rapid localization of the SPF during TESPAL.

METHODS

We reviewed computed tomography (CT) of the sinus from 50 adult patients who presented to a tertiary care outpatient rhinology clinic. Helical CTs were performed according to a standard clinical protocol in

From the Department of Otolaryngology—Head and Neck Surgery, University of Colorado School of Medicine, Aurora, Colorado

No funding sources supported research

The authors have no conflicts of interest to declare pertaining to this article

Address correspondence to Vijay R. Ramakrishnan, M.D., Department of Otolaryngology—Head and Neck Surgery, University of Colorado, 12631 E. 17th Ave., B205, Aurora, CO 80045

E-mail address: vijay.ramakrishnan@ucdenver.edu

This work is published and licensed by OceanSide Publications, Inc. The full terms of this license are available at <https://www.allergyandrhinology.com/terms> and incorporate the Creative Commons License Deed: Attribution – Non-Commercial – NoDerivs 4.0 Unported (CC BY-NC-ND 4.0). By accessing the work you hereby accept the terms. Non-commercial uses of the work are permitted without any further permission from OceanSide Publications, Inc., provided the work is properly attributed. Any use of the work other than as authorized under this license or copyright law is prohibited. Copyright © 2017, OceanSide Publications, Inc., U.S.A.

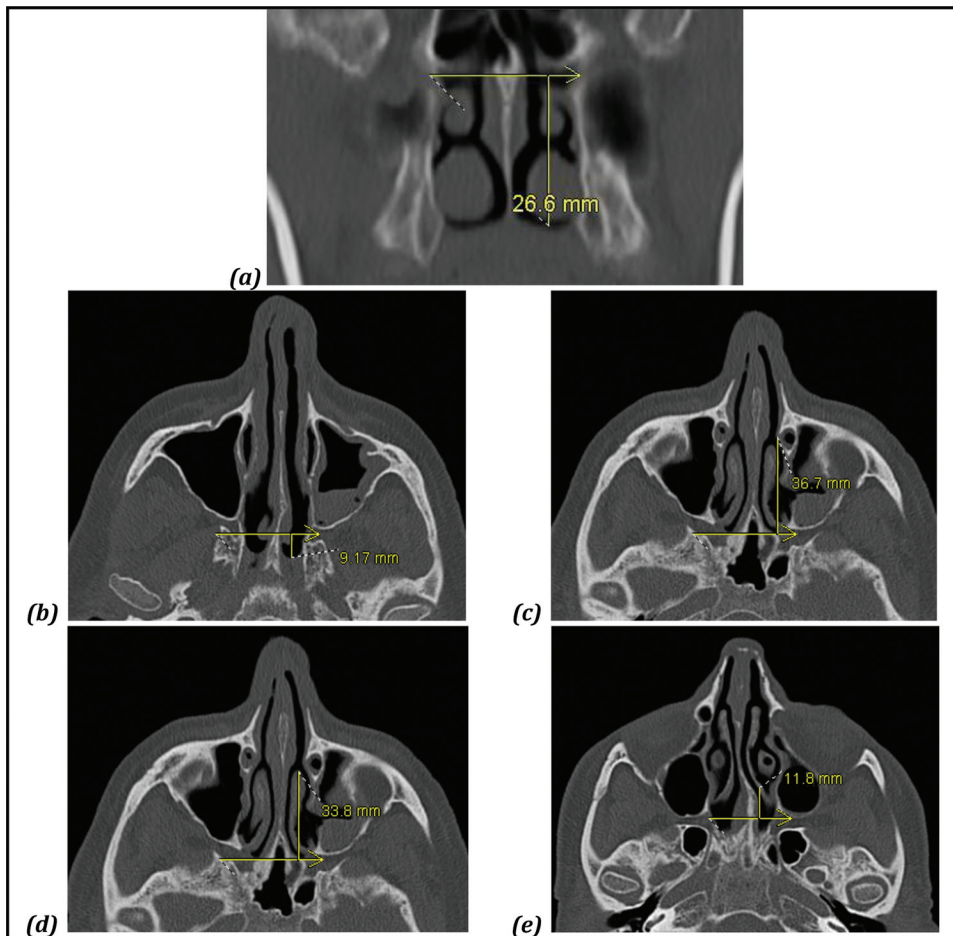


Figure 1. Representative computed tomography measurements from each landmark to the sphenopalatine foramen (SPF). (a) Nasal floor; (b) choanal arch; (c) maxillary line; (d) anterior head of the middle turbinate; and (e) basal lamella.

which 1-mm images are acquired, and 1-mm and 3-mm axial and coronal reconstructions, respectively, are created. Patients with evidence of previous sinus, nasal, or skull base surgery, or those with significant obscuring sinonasal pathology were excluded. Institutional review board approval was obtained for this study (COMIRB 13-1555). The distances from the SPF to the following surgical landmarks were measured from each side⁸: nasal floor, choanal arch, maxillary line, anterior head of the middle turbinate, and the basal lamella of the middle turbinate (Fig. 1). These landmarks were selected for their consistent and reliable identification during nasal endoscopy and CT examination. Both axial and coronal CT sinus images were reviewed to locate each landmark, and the distances were measured by using the ruler function of McKesson Radiology Station software (Alpharetta, GA). Distances to the SPF in the anteroposterior dimension were recorded for all except the nasal floor, which was recorded in the vertical dimension. Mean distances and standard deviations (SD) were calculated; laterality and sex group comparisons were made by using paired and unpaired two-tailed Student's *t*-test, respectively (Excel version 2008; Microsoft; Redmond, WA).

RESULTS

Fifty adult patients were included, for a total of 500 measurements. The mean age was 47.5 years (range, 18–78 years), with a 1:1 male-female ratio. Right- and left-sided measurements were pooled for subsequent comparisons, given their similarity on paired *t*-test ($p = 0.79$) and small SDs. Distances between the anatomic landmarks and the SPF are displayed in Table 1. The mean (SD) SPF was 26.6 ± 2.6 mm above the nasal floor, as measured in the vertical dimension. In the anteroposterior dimension, the mean (SD) SPF measured 36.7 ± 5.5 mm deep to the maxillary line, 33.8 ± 6.7 mm deep to the anterior head of the middle turbinate, 11.8 ± 1.9 mm deep to the level of the basal lamella, and 9.2 ± 1.4 mm anterior to the choanal arch. The distances were ~ 1 – 3 mm greater in male than female patients, with the exception of the distance from the basal lamella to the SPF. These distances are depicted in the included anatomic illustration (Fig. 2).

DISCUSSION

Intractable posterior epistaxis may be managed with either arterial ligation or embolization of the SPA because these procedures have higher patient satisfac-

Table 1 Distances from landmarks to the SPF

	Distance to SPF, mean \pm SD, mm			<i>p</i> Value
	Overall	Men	Women	
Nasal floor	26.6 \pm 2.6	27.3 \pm 3.0	25.9 \pm 2.0	0.01
Choanal arch	-9.2 \pm 1.4	-9.5 \pm 1.3	-8.9 \pm 1.4	0.01
Maxillary line	36.7 \pm 5.5	38.2 \pm 5.3	35.3 \pm 5.3	0.01
Ant middle turb	33.8 \pm 6.7	35.3 \pm 5.9	32.3 \pm 7.2	0.03
Basal lamella	11.8 \pm 1.9	11.8 \pm 1.7	11.8 \pm 2.0	0.89

SD = Standard deviation; SPF = sphenopalatine foramen; Ant middle turb = anterior head of the middle turbinate. The *p* values are shown for male-to-female comparison.

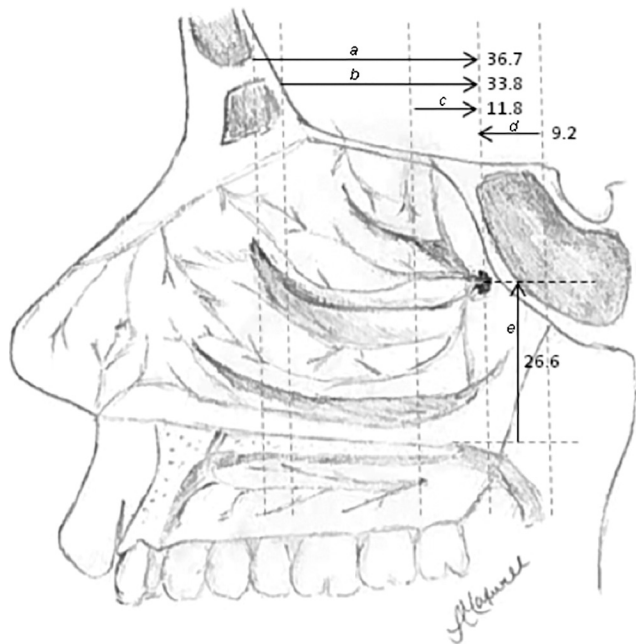


Figure 2. Schematic of endoscopic measurements to sphenopalatine foramen (SPF) in millimeters. Measurements a–d are in the anteroposterior dimension, and measurement e is in the vertical dimension. (a) Maxillary line to SPF; (b) anterior head of the middle turbinate to SPF; (c) basal lamella to SPF; (d) arch of choana to SPF; and (e) nasal floor to SPF.

tion, increased efficacy, and cost savings when compared with traditional posterior packing and observation.^{4,6,7} As an alternative to surgical intervention, transcatheter embolization remains a reasonable choice for poor surgical candidates or when surgical expertise is not available. However, rare but devastating risks accompany embolization procedures, including stroke, facial pain and paresthesias, ophthalmoplegia, blindness, and soft-tissue necrosis, all while carrying a higher recurrence rate for epistaxis (~20%) than TESPAL procedures.^{6,7}

The preferred surgical procedure for epistaxis management has evolved over time. Previous surgical methods to control posterior epistaxis relied on

transantral ligation of the IMA; however, this procedure has been associated with significant morbidity, including sinusitis, facial pain or edema, infraorbital nerve paresthesia, and oroantral fistula.^{7,9–11} In addition, pterygopalatine fossa dissection carries rare risks of blindness, ophthalmoplegia, decreased lacrimation, and hematoma⁷; and, yet, transantral IMA ligation still carries an ~10% rate of recurrent epistaxis.^{6,7}

A microsurgical approach to SPA ligation was first described by Prades¹² in 1976, and later Budrovich and Saetti¹³ described the endoscopic approach to SPA ligation. Since then, this has become the procedure of choice due to its efficacy, rarity of minor complications, and cost-effectiveness.^{1,4,6,7,13} The procedure is fairly straightforward, relying on localization of the crista ethmoidalis anterior to the SPF, visualizing the artery as it exits the foramen, and searching for nearby accessory branches. Generally, a mucosal incision is made on the lateral nasal wall anterior to the middle turbinate basal lamella insertion, and elevation of the mucoperiosteal flap is performed until the crista ethmoidalis and SPF are found within the superior meatus. An optional maxillary antrostomy can be performed to help delineate the boundary between the posterior fontanelle and the palatine bone, and demonstrate the depth required to reach the pterygopalatine fossa.

Difficulty locating the SPF can occur during active hemorrhage, when medical anticoagulation is still present, or with the mucosal friability after multiple rounds of nasal packing or recent attempts at surgical management. Although previous studies identified anatomic variations that resulted in controversy regarding the location of the SPF, it is generally found superior to the posterior attachment of the middle turbinate in the region of the superior meatus.^{1,8,14} Based on our measurements, we proposed using the expected distances from simple endoscopic landmarks to the SPF to triangulate the most likely location of the SPA. The radiographic measurements described in this study may be used to guide incision placement and elevate a

smaller flap directly onto the foramen or coagulate directly on top of it.

The anatomic landmarks in this study were chosen for easy identification during nasal endoscopy and their expected presence, even in the setting of previous surgery or trauma. Distances were greater in male patients for most measurements, consistent with the larger mean nasal cavity dimensions typically seen in men.¹⁵ The choanal arch and basal lamella are the most reliable landmarks, as evidenced by their small SDs, possibly due to their close proximity to the SPF. This indicates that the quickest initial way to estimate the location of the foramen in initial nasal endoscopy is to first identify the basal lamella and the arch of the choana. By estimating the midpoint between the basal lamella and choanal arch, the anteroposterior depth of the foramen can be established. The foramen is located 2.5 cm up from the nasal floor, which can be estimated by using the diameter of the suction tip (Fig. 2).

Limitations of this study included a possible selection bias and challenges in using two-dimensional measurements in a three-dimensional space. The subjects presented with sinus concerns to undergo CTs, and we did not compare these with a healthy control group. However, previous studies indicate no major anatomic predisposing factors for rhinosinusitis, which made this an unlikely issue.^{16,17} Also, these distances were measured on two-dimensional CT images, and if these were not true axial and coronal planes, then measurements would be slightly off. To minimize this possibility, CTs with direct thin-cut (≤ 1 mm) axial acquisition protocols were used and the nasal floor was used to confirm the true nature of the axial plane. If a few degrees of tilt were still present despite this visual examination, with measurements of 9–37 mm, then very little difference in absolute measurement would occur. Use of these measurements is not a substitute for detailed anatomic knowledge, which is essential for any surgeon. The mean distances described can serve as a useful tool for localization of the region of the SPF and can facilitate rapid surgical exposure.

CONCLUSION

Radiographic analysis of both sexes demonstrated reliable endoscopic landmarks that could be used to

estimate the location of the SPF, with slightly larger nasal cavity volumes observed in men.

REFERENCES

1. Rudmik L, and Smith TL. Management of intractable spontaneous epistaxis. *Am J Rhinol Allergy* 26:55–60, 2012.
2. Hadoura L, Douglas C, McGarry GW, and Young D. Mapping surgical coordinates of the sphenopalatine foramen: Surgical navigation study. *J Laryngol Otol* 123:742–745, 2009.
3. Feusi B, Holzmann D, and Steurer J. Posterior epistaxis: Systematic review on the effectiveness of surgical therapies. *Rhinology* 43:300–304, 2005.
4. Douglas R, and Wormald PJ. Update on epistaxis. *Curr Opin Otolaryngol Head Neck Surg* 15:180–183, 2007.
5. Loughran S, Hilmi O, and McGarry GW. Endoscopic sphenopalatine artery ligation—When, why and how to do it. An on-line video tutorial. *Clin Otolaryngol* 30:539–543, 2005.
6. Seno S, Arikata M, Sakurai H, et al. Endoscopic ligation of the sphenopalatine artery and the maxillary artery for the treatment of intractable posterior epistaxis. *Am J Rhinol Allergy* 23:197–199, 2009.
7. Schwartzbauer HR, Shete M, and Tami TA. Endoscopic anatomy of the sphenopalatine and posterior nasal arteries: Implications for the endoscopic management of epistaxis. *Am J Rhinol* 17:63–66, 2003.
8. Lund VJ, Stammberger H, Fokkens WJ, et al. European position paper on the anatomic terminology of the internal nose and paranasal sinuses. *Rhinology* 50(suppl. 24):1:34, 2014.
9. Chandler JR, and Serrins AJ. Transantral ligation of the internal maxillary artery for epistaxis. *Laryngoscope* 75:1151–1159, 1965.
10. McDonald TJ, and Pearson BW. Follow-up on maxillary artery ligation for epistaxis. *Arch Otolaryngol* 106:635–638, 1980.
11. Kumar S, Shetty A, Rockey J, and Nilssen E. Contemporary surgical treatment of epistaxis. What is the evidence for sphenopalatine artery ligation? *Clin Otolaryngol Allied Sci* 28:360–363, 2003.
12. Prades J. Abord endonasal de la fossa pterygo-mexilaire. LXXIII Congres Francais d’Oto-Rhino-Laryngologie: Rendus des seanc, 290–296, 1976.
13. Budrovich R, and Saetti R. Microscopic and endoscopic ligation of the sphenopalatine artery. *Laryngoscope* 102(pt. 1):1391–1394, 1992.
14. Wareing MJ, and Padgham ND. Osteologic classification of the sphenopalatine foramen. *Laryngoscope* 108(pt. 1):125–127, 1998.
15. Samoliński BK, Grzanka A, and Gotlib T. Changes in nasal cavity dimensions in children and adults by gender and age. *Laryngoscope* 117:1429–1433, 2007.
16. Kim HJ, Jung Cho M, Lee JW, et al. The relationship between anatomic variations of paranasal sinuses and chronic sinusitis in children. *Acta Otolaryngol* 126:1067–1072, 2006.
17. Nouraei SA, Elisay AR, Dimarco A, et al. Variations in paranasal sinus anatomy: Implications for the pathophysiology of chronic rhinosinusitis and safety of endoscopic sinus surgery. *J Otolaryngol Head Neck Surg* 38:32–37, 2009. □